Available online at www.sciencedirect.com

ScienceDirect

Procedia Structural Integrity 28 (2020) 464–471

Structural Integrity Procedia

www.elsevier.com/locate/procedia

1st Virtual European Conference on Fracture

# Peridynamic formulation for Timoshenko beam

Zhenghao Yang[a,*], Selda Oterkus[a], Erkan Oterkus[a]

[a]*PeriDynamics Research Centre, Department of Naval Architecture, Ocean and Marine Engineering, University of Strathclyde, 100 Montrose Street, Glasgow G4 0LZ, UK*

**Abstract**

It is common to encounter structures with complex geometries including aerospace and ship structures. Moreover, in these structures one dimension can be either much smaller or bigger than other two dimensions. In such cases, special formulations were developed such as beam, plate and shell formulations. These formulations are available both in classical and non-classical frameworks. In this study, a new peridynamic formulation is presented for Timoshenko beams. Peridynamic equations are obtained by using Euler-Lagrange equations and Taylor's expansion. To validate the newly developed peridynamic formulation, a Timoshenko beam subjected to central point load under simply supported, clamped and mixed (clamped-simply supported) boundary conditions is considered. Peridynamic results are compared against finite element analysis solutions and a very good agreement is observed between the two solutions.



*Keywords:* Peridynamics; Timoshenko beam; Euler-Lagrange equation; Non-local

## 1. Introduction

It is common to encounter structures with complex geometries including aerospace and ship structures. Moreover, in these structures one dimension can be either much smaller or bigger than other two dimensions. In such cases, special formulations were developed such as beam, plate and shell formulations. These formulations are available both

* Corresponding author. Tel.: +44-141-548-3876.
*E-mail address:* zhenghao.yang@strath.ac.uk


10.1016/j.prostr.2020.10.055

in classical and non-classical frameworks. In this study, a new Timoshenko beam formulation is presented within peridynamic framework. Peridynamics (PD) is a new continuum mechanics formulation within the class of non-local continuum mechanics. PD was introduced by Silling (2000) and it is especially suitable for predicting failure. Moreover, it has a length scale parameter called horizon so that non-local effects can be captured. Especially during the recent years, there has been a rapid progress on peridynamics research. Amongst these Imachi et al. (2019) developed a new transition bond concept for dynamic fracture analysis which was then used for dynamic crack arrest analysis (Imachi et al., 2020). Kefal et. al. (2019) utilized peridynamics for topology optimization of cracked structures. De Meo et. al. (2016) and Zhu et. al. (2016) studied granular fracture in polycrystalline materials by using peridynamics. Oterkus et. al. (2012) performed peridynamic impact damage assessment of reinforced concrete. It is also possible to perform fatigue analysis within peridynamic framework as demonstrated in Oterkus et. al. (2010b). Anisotropic materials such as composites can be analyzed by utilizing peridynamics (Oterkus et. al. 2010a; Oterkus and Madenci 2012a,b). Peridynamics is also suitable for analysis of nanostructures including graphene (Liu et. al. 2018). Microcrack-macrocrack interactions is another important problem of interest in fracture mechanics which was studied by Vazic et. al. (2017) and Basoglu et. al. (2019) by using peridynamics. Peridynamics is not limited to structural analysis and can be used for other fields. To perform damage analysis in Lithium-Ion batteries, Wang et. al. (2018) developed a coupled diffusion-mechanical model to predict fracture evolution during lithiation process. Moisture is an important concern for electronic packages and Diyaroglu et. al. (2017b) presented peridynamic wetness approach for moisture diffusion analysis. In addition, Oterkus et. al. (2014) performed peridynamic hygro-thermo-mechanical analysis to predict failure in electronic packages. In another study, Diyaroglu et. al. (2017a) demonstrated how to perform peridynamic diffusion analysis in a commercial finite element software. De Meo et al. (2017) presented a peridynamic pitting corrosion damage model which was then further studied by De Meo et. al. (2017) to predict crack initiation and propagation from corrosion pits.

As the main focus of this study, peridynamics has also been utilized to model beam, plate and shell type simplified structures. O'Grady and Foster developed a non-ordinary state-based peridynamic beam model suitable for Euler beams. In another study, Diyaroglu et al. (2019) presented Euler beam formulation in ordinary state-based framework. As an extension of this study, Yang et. al. (2020) introduced a new Kirchhoff plate formulation in state-based peridynamic framework. Taylor and Steigmann (2015) developed a two-dimensional peridynamic model for thin plates. Vazic et. al. (2020) proposed a peridynamic model suitable for Mindlin plates resting on a Winkler foundation. In this study, a new peridynamic formulation is presented for Timoshenko beams. The formulation is obtained by using Euler-Lagrange equation. Several benchmark cases are considered for different boundary conditions and peridynamic solutions are compared against finite element method results.

## 2. Classical Timoshenko Beam Formulation

According to classical Timoshenko beam theory, the displacement components of a material point in axial ($x$) and transverse ($z$) directions, $u$ and $w$, respectively, can be expressed in terms of transverse displacement and rotation of the material points along the central axis, $\overline{w}$ and $\overline{\theta}$, as

$$u(x,z,t) = z\theta(x,0,t) = z\overline{\theta} \tag{1a}$$

$$w(x,z,t) = w(x,0,t) = \overline{w} \tag{1b}$$

By using the definitions given in Eqs. (1a,b), strain components can be defined as

$$\varepsilon_{xx} = z\frac{\partial\overline{\theta}}{\partial x} \tag{2a}$$

$$\gamma_{xz} = \overline{\theta} + \frac{\partial\overline{w}}{\partial x} \tag{2b}$$

$$\varepsilon_{zz} = 0 \tag{2c}$$

Next, the stress components for Timoshenko beam can be written as

$$\sigma_{xx} = E\varepsilon_{xx} = Ez\frac{\partial\bar{\theta}}{\partial x} \tag{3a}$$

$$\tau_{xz} = G\left(\bar{\theta} + \frac{\partial\bar{w}}{\partial x}\right) \tag{3b}$$

where $E$ and $G$ are elastic and shear moduli, respectively. The strain energy of a material point, $W$ , can obtained by using the stress and strain expressions given in Eqs. (2a-c) and (3a,b) as

$$W = \frac{1}{2}\left(\sigma_{xx}\varepsilon_{xx} + \tau_{xz}\gamma_{xz}\right) = \frac{1}{2}\left\{Ez^2\left(\frac{\partial\bar{\theta}}{\partial x}\right)^2 + \kappa G\left(\bar{\theta} + \frac{\partial\bar{w}}{\partial x}\right)^2\right\} \tag{4}$$

where $\kappa$ is the shear correction factor. The average strain energy density can be calculated by integrating the strain energy density expression given in Eq. (4) throughout the cross-sectional area and dividing by the cross-sectional area, $A$ , as

$$\bar{W} = \frac{1}{A}\int_A W dA = \frac{1}{2A}\left\{EI\left(\frac{\partial\bar{\theta}}{\partial x}\right)^2 + \kappa GA\left(\bar{\theta} + \frac{\partial\bar{w}}{\partial x}\right)^2\right\} \tag{5}$$

where $I$ is the moment of inertia.

## 3. Peridynamic Timoshenko Beam Formulation

The peridynamic equation of motion for a Timoshenko beam can be obtained by using Euler-Lagrange equation and can be written for a particular material point $k$ as

$$\frac{d}{dt}\frac{\partial L}{\partial\dot{\mathbf{q}}_{(k)}} - \frac{\partial L}{\partial\mathbf{q}_{(k)}} = 0 \tag{6}$$

with the Lagrangian,

$$L = T - U \tag{7a}$$

and degrees of freedom

$$\mathbf{q}_{(k)} = \begin{Bmatrix}\bar{\theta}_{(k)} \\ \bar{w}_{(k)}\end{Bmatrix} \tag{7b}$$

The total kinetic and potential energy of the beam can be calculated, respectively, as

$$T = \frac{1}{2}\sum_k \rho_{(k)}\left(\frac{I}{A}\dot{\bar{\theta}}_{(k)}^2 + \dot{\bar{w}}_{(k)}^2\right)V_{(k)} \tag{8a}$$

$$U = \sum_k \bar{W}_{(k)}V_{(k)} - \sum_k\left(\mathbf{b}_{(k)}\cdot\mathbf{q}_{(k)}\right)V_{(k)} \tag{8b}$$

where $\rho_{(k)}$ is the density, $V_{(k)}$ is the volume and the body load vector, $\mathbf{b}_{(k)}$, is defined as

$$\mathbf{b}_{(k)} = \begin{Bmatrix} b_{\theta(k)} \\ b_{w(k)} \end{Bmatrix} \tag{9}$$

To obtain the peridynamic equation of motion, the classical strain energy density expression given in Eqs. (4) and (5) should be converted into a peridynamic form. This can be achieved by using Taylor's expansions and the following relationships can be obtained

$$\left(\frac{\partial \bar{\theta}_{(k)}}{\partial x}\right)^2 = \frac{1}{\delta^2 A}\sum_i \frac{\left(\bar{\theta}_{(i^k)} - \bar{\theta}_{(k)}\right)^2}{\left|\xi_{(i^k)(k)}\right|} V_{(i^k)} \tag{10a}$$

$$\left(\frac{\partial \bar{w}_{(k)}}{\partial x} + \bar{\theta}_{(k)}\right)^2 = \frac{1}{\delta^2 A}\sum_i \frac{\left(\bar{w}_{(i^k)} - \bar{w}_{(k)} + \frac{\bar{\theta}_{(i^k)} + \bar{\theta}_{(k)}}{2}\xi_{(i^k)(k)}\right)^2}{\left|\xi_{(i^k)(k)}\right|} V_{(i^k)} \tag{10b}$$

where $\delta$ is the horizon size and $A$ is the cross-sectional area. By substituting the definitions given in Eqs. (10a,b) into Eq. (5) yields the strain energy densities of the material point *k* and the material point inside its horizon *j* as

$$\bar{W}_{(k)} = \frac{1}{2}\frac{1}{\delta^2 A^2}\left\{ EI\sum_i \frac{\left(\bar{\theta}_{(i^k)} - \bar{\theta}_{(k)}\right)^2}{\left|\xi_{(i^k)(k)}\right|} V_{(i^k)} + \kappa GA \sum_i \frac{\left(\bar{w}_{(i^k)} - \bar{w}_{(k)} + \frac{\bar{\theta}_{(i^k)} + \bar{\theta}_{(k)}}{2}\xi_{(i^k)(k)}\right)^2}{\left|\xi_{(i^k)(k)}\right|} V_{(i^k)} \right\} \tag{11a}$$

$$\bar{W}_{(j)} = \frac{1}{2}\frac{1}{\delta^2 A^2}\left\{ EI\sum_i \frac{\left(\bar{\theta}_{(i^j)} - \bar{\theta}_{(j)}\right)^2}{\left|\xi_{(i^j)(j)}\right|} V_{(i^j)} + \kappa GA \sum_i \frac{\left(\bar{w}_{(i^j)} - \bar{w}_{(j)} + \frac{\bar{\theta}_{(i^j)} + \bar{\theta}_{(j)}}{2}\xi_{(i^j)(j)}\right)^2}{\left|\xi_{(i^j)(j)}\right|} V_{(i^j)} \right\} \tag{11b}$$

By using Eqs. (8a,b) and (11a,b), the peridynamic equations of motion of Timoshenko beam can be obtained from Euler-Lagrange equation given in Eq. (6) as

$$\rho_{(k)}\frac{I}{A}\ddot{\bar{\theta}}_{(k)} = c_b \sum_j \frac{\left(\bar{\theta}_{(j)} - \bar{\theta}_{(k)}\right)^2}{\left|\xi_{(j)(k)}\right|} V_{(j)} - \frac{1}{2}c_s \sum_j \left(\bar{w}_{(j)} - \bar{w}_{(k)} + \frac{\bar{\theta}_{(j)} + \bar{\theta}_{(k)}}{2}\xi_{(j)(k)}\right) sign\left(\xi_{(j)(k)}\right) V_{(j)} + b_{\theta(k)} \tag{12a}$$

$$\rho_{(k)}\ddot{\bar{w}}_{(k)} = c_s \sum_j \left(\frac{\bar{w}_{(j)} - \bar{w}_{(k)}}{\left|\xi_{(j)(k)}\right|} + \frac{\bar{\theta}_{(j)} + \bar{\theta}_{(k)}}{2} sign\left(\xi_{(j)(k)}\right)\right) V_{(j)} + b_{w(k)} \tag{12b}$$

with

$$c_b = \frac{2EI}{A^2\delta^2} \tag{13a}$$

$$c_s = \frac{2\kappa G}{A\delta^2} \tag{13b}$$

## 4. Numerical results

In order to validate the current peridynamic Timoshenko beam formulation, several different benchmark problems were considered for a beam subjected to central loading under simply supported, clamped and mixed (clamped-simply supported) boundary conditions. Peridynamic solutions were compared against finite element analysis results.

### *4.1. Simply supported beam subjected to a central point force*

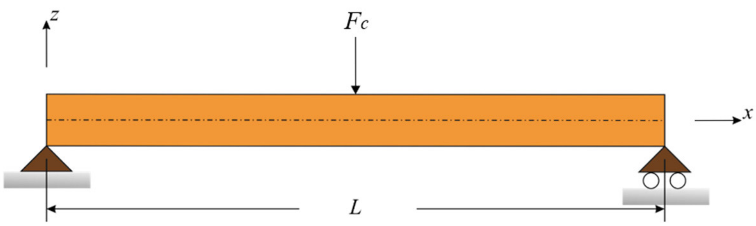


Fig. 1. Simply supported beam subjected to a central point force.

In the first example case, a Timoshenko beam having 1 m length, 0.05 m width and 0.1 m thickness is considered as shown in Fig. 1. The elastic modulus and Poisson's ratio are specified as 200 GPa and 0.3, respectively. The shear correction factor is specified as $\kappa = 5/6$. For spatial discretization, a discretization size of $\Delta = 0.002\,\text{m}$ is utilized. The horizon size is chosen as $\delta = 3\Delta$. The steady-state solution is obtained by using adaptive dynamic relaxation scheme presented in Kilic and Madenci (2010). A point load of $F = 100\,N$ is applied at the center of the beam as a body load. The simply supported boundary conditions were applied by introducing fictitious regions both at the left and right edges. Finite element analysis (FEA) solution was obtained by using ANSYS, a commercial finite element software. Finite element model was created by using 100 BEAM188 elements along the beam.

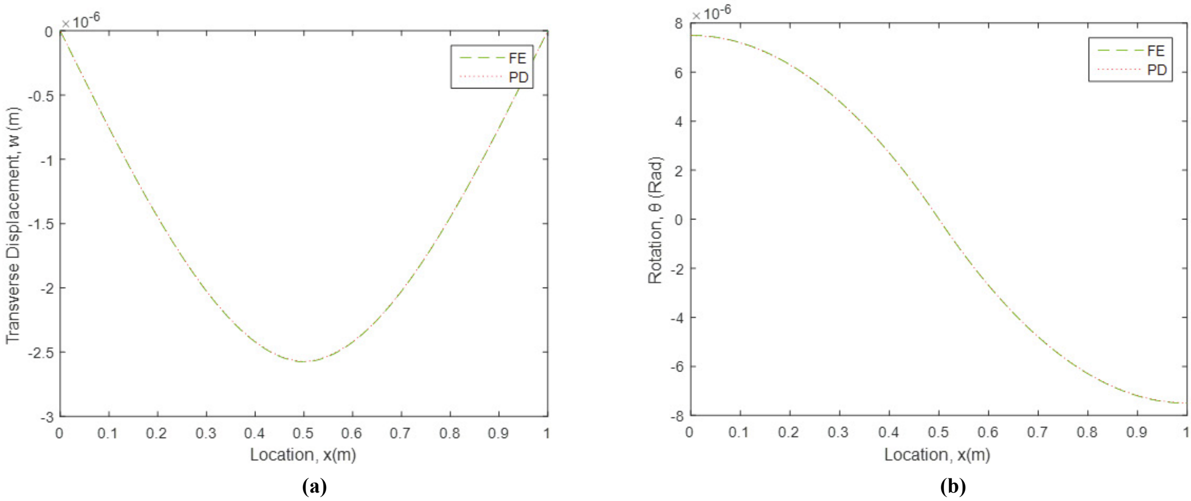


Fig. 2. Variation of (a) transverse displacement, (b) rotation along the beam (PD: Peridynamics, FE: Finite Element Analysis).

Variation of transverse displacement and rotation along the beam is shown in Fig. 2. PD results are compared against FEA results and a very good agreement is observed between the two solutions.

### *4.2. Clamped beam subjected to a central point force*

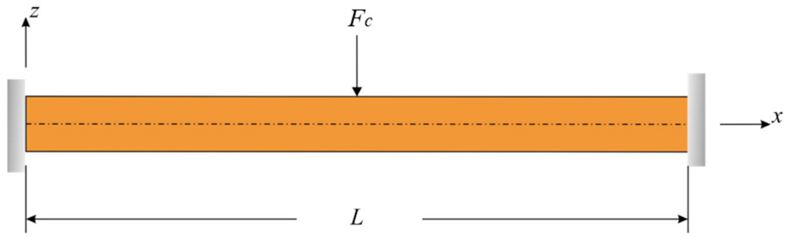


Fig. 3. Clamped beam subjected to a central point force.

In the second example case, as shown in Fig. 3, the simply-supported boundary conditions were replaced with clamped boundary conditions at both right and left edges. Variation of transverse displacement and rotation along the beam is depicted in Fig. 4 and a very good agreement was obtained between PD and FEA results.

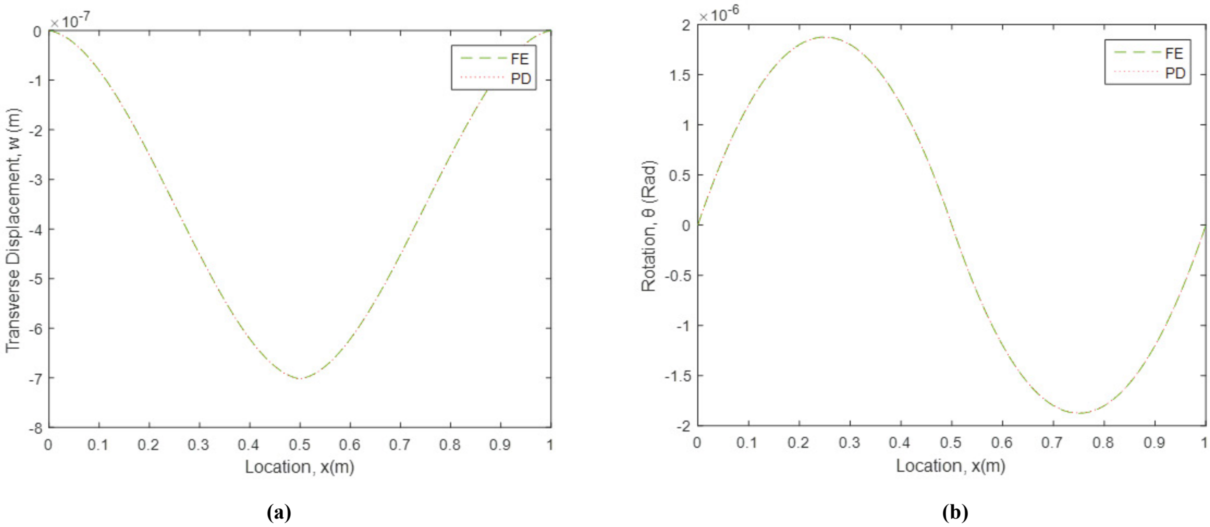


Fig. 4. Variation of (a) transverse displacement, (b) rotation along the beam (PD: Peridynamics, FE: Finite Element Analysis).

### *4.3. Beam subjected to a central point force and mixed boundary conditions*

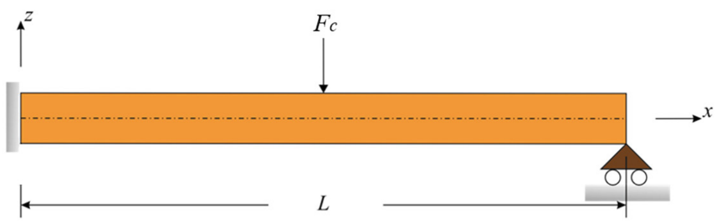


Fig. 5. Beam subjected to a central point force and mixed boundary conditions.

In the last example case, a mixed boundary condition was considered by assigning clamped boundary condition at the left edge and simply supported boundary condition at the right edge as shown in Fig. 5. Variation of transverse displacement and rotation results along the beam was compared between PD and FEA results. As depicted in Fig. 6, a very good match was observed between the two approaches.

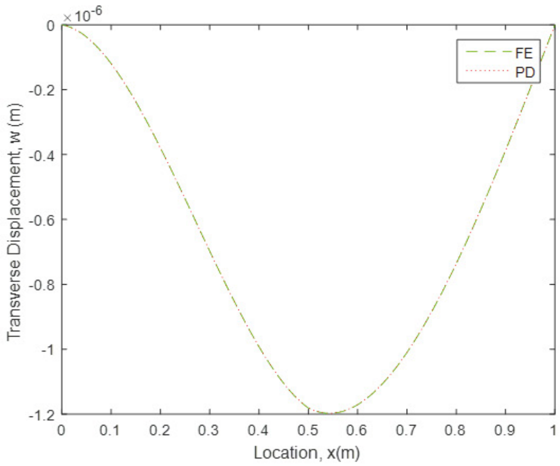


**(a)**

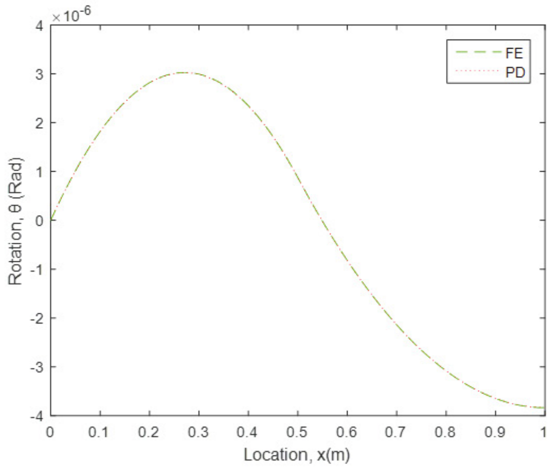


**(b)**

Fig. 6. Variation of (a) transverse displacement, (b) rotation along the beam (PD: Peridynamics, FE: Finite Element Analysis).

## 5. Conclusions

In this study, a new peridynamic formulation was presented for Timoshenko beams. Peridynamic equations were obtained by using Euler-Lagrange equations and Taylor's expansion. To validate the newly developed peridynamic formulation, a Timoshenko beam subjected to central point load under simply supported, clamped and mixed (clamped-simply supported) boundary conditions was considered. Peridynamic results were compared against finite element analysis solutions and a very good agreement was observed between the two solutions.

## References

Basoglu, M.F., Zerin, Z., Kefal, A., Oterkus, E., 2019. A computational model of peridynamic theory for deflecting behavior of crack propagation with micro-cracks. Computational Materials Science 162, 33–46.
De Meo, D., Zhu, N., Oterkus, E., 2016. Peridynamic modeling of granular fracture in polycrystalline materials. Journal of Engineering Materials and Technology 138(4), 041008.
De Meo, D., Oterkus, E., 2017. Finite element implementation of a peridynamic pitting corrosion damage model. Ocean Engineering 135, 76–83.
De Meo, D., Russo, L., Oterkus, E., 2017. Modeling of the onset, propagation, and interaction of multiple cracks generated from corrosion pits by using peridynamics. Journal of Engineering Materials and Technology 139(4), 041001.
Diyaroglu, C., Oterkus, S., Oterkus, E., Madenci, E., 2017. Peridynamic modeling of diffusion by using finite-element analysis. IEEE Transactions on Components, Packaging and Manufacturing Technology 7(11), 1823–1831.
Diyaroglu, C., Oterkus, S., Oterkus, E., Madenci, E., Han, S., Hwang, Y., 2017. Peridynamic wetness approach for moisture concentration analysis in electronic packages. Microelectronics Reliability 70, 103–111.
Diyaroglu, C., Oterkus, E., Oterkus, S., 2019. An Euler–Bernoulli beam formulation in an ordinary state-based peridynamic framework. Mathematics and Mechanics of Solids 24(2), 361–376.
Imachi, M., Tanaka, S., Bui, T.Q., Oterkus, S., Oterkus, E., 2019. A computational approach based on ordinary state-based peridynamics with new transition bond for dynamic fracture analysis. Engineering Fracture Mechanics 206, 359–374.
Imachi, M., Tanaka, S., Ozdemir, M., Bui, T.Q., Oterkus, S., Oterkus, E., 2020. Dynamic crack arrest analysis by ordinary state-based peridynamics. International Journal of Fracture 221(2), pp.155–169.
Kefal, A., Sohouli, A., Oterkus, E., Yildiz, M., Suleman, A., 2019. Topology optimization of cracked structures using peridynamics. Continuum Mechanics and Thermodynamics 31(6), 1645–1672.
Kilic, B., Madenci, E., 2010. An adaptive dynamic relaxation method for quasi-static simulations using the peridynamic theory. Theoretical and Applied Fracture Mechanics 53(3), 194–204.
Liu, X., He, X., Wang, J., Sun, L., Oterkus, E., 2018. An ordinary state-based peridynamic model for the fracture of zigzag graphene sheets. Proceedings of the Royal Society A: Mathematical, Physical and Engineering Sciences 474(2217), p.20180019.
Madenci, E., Oterkus, E., 2014. Peridynamic theory. Springer, New York, NY.

O'Grady, J., Foster, J., 2014. Peridynamic beams: a non-ordinary, state-based model. International Journal of Solids and Structures 51(18), 3177–3183.
Oterkus, E., Barut, A., Madenci, E., 2010a. Damage growth prediction from loaded composite fastener holes by using peridynamic theory. In 51st AIAA/ASME/ASCE/AHS/ASC Structures, Structural Dynamics, and Materials Conference 18th AIAA/ASME/AHS Adaptive Structures Conference, Orlando, Florida, USA, p. 3026.
Oterkus, E., Guven, I. and Madenci, E., 2010b. Fatigue failure model with peridynamic theory. In 12th IEEE Intersociety Conference on Thermal and Thermomechanical Phenomena in Electronic Systems, Las Vegas, Nevada, USA, p. 1-6.
Oterkus, E., Madenci, E., 2012a. Peridynamics for failure prediction in composites. In 53rd AIAA/ASME/ASCE/AHS/ASC Structures, Structural Dynamics and Materials Conference 20th AIAA/ASME/AHS Adaptive Structures Conference, Honolulu, Hawaii, USA, p. 1692.
Oterkus, E., Madenci, E., 2012b. Peridynamic theory for damage initiation and growth in composite laminate. Key Engineering Materials 488, 355–358.
Oterkus, E., Guven, I., Madenci, E., 2012. Impact damage assessment by using peridynamic theory. Open Engineering 2(4), 523–531.
Oterkus, S., Madenci, E., Oterkus, E., Hwang, Y., Bae, J., Han, S., 2014, May. Hygro-thermo-mechanical analysis and failure prediction in electronic packages by using peridynamics. In 2014 IEEE 64th Electronic Components and Technology Conference (ECTC), Orlando, Florida, USA, p. 973-982.
Silling, S.A., 2000. Reformulation of elasticity theory for discontinuities and long-range forces. Journal of the Mechanics and Physics of Solids 48(1), 175–209.
Taylor, M., Steigmann, D.J., 2015. A two-dimensional peridynamic model for thin plates. Mathematics and Mechanics of Solids 20(8), 998–1010.
Vazic, B., Wang, H., Diyaroglu, C., Oterkus, S., Oterkus, E., 2017. Dynamic propagation of a macrocrack interacting with parallel small cracks. AIMS Materials Science 4(1), pp.118–136.
Vazic, B., Oterkus, E., Oterkus, S., 2020. Peridynamic model for a Mindlin plate resting on a Winkler elastic foundation. Journal of Peridynamics and Nonlocal Modeling, pp.1–10.
Wang, H., Oterkus, E., Oterkus, S., 2018. Predicting fracture evolution during lithiation process using peridynamics. Engineering Fracture Mechanics 192, 176–191.
Yang, Z., Oterkus, E., Nguyen, C.T., Oterkus, S., 2019. Implementation of peridynamic beam and plate formulations in finite element framework. Continuum Mechanics and Thermodynamics 31(1), 301–315.
Yang, Z., Vazic, B., Diyaroglu, C., Oterkus, E., Oterkus, S., 2020. A Kirchhoff plate formulation in a state-based peridynamic framework. Mathematics and Mechanics of Solids 25(3), 727–738.
Zhu, N., De Meo, D., Oterkus, E., 2016. Modelling of granular fracture in polycrystalline materials using ordinary state-based peridynamics. Materials 9(12), p.977.